BIOCHEMISTRY
including biophysical chemistry & molecular biology

Article

pubs.acs.org/biochemistry

Interaction of Fibrin with the Very Low Density Lipoprotein Receptor: Further Characterization and Localization of the Fibrin-Binding Site

Sergiy Yakovlev and Leonid Medved*

Center for Vascular and Inflammatory Diseases and Department of Biochemistry and Molecular Biology, University of Maryland School of Medicine, Baltimore, Maryland 21201, United States

ABSTRACT: Our recent study revealed that fibrin interacts with the very low density lipoprotein receptor (VLDLR) on endothelial cells through its βN domains, and this interaction promotes transendothelial migration of leukocytes and thereby inflammation. The major aims of this study were to further characterize this interaction and localize the fibrin-binding site in the VLDLR. To localize the fibrin-binding site, we expressed a soluble extracellular portion of this receptor, $sVLDLR_{HT}$, its N- and C-terminal regions, $VLDLR(1-8)_{HT}$ and $des(1-8)VLDLR_{HT}$, respectively, and a number of VLDLR fragments containing various combinations of CR domains and confirmed their proper folding by fluorescence spectroscopy. Interaction of these fragments with the $(\beta 15-66)_2$ fragment corresponding to a pair of VLDLR-binding βN domains of fibrin was tested by different methods. Our experiments performed by an enzyme-linked immunosorbent assay and surface plasmon resonance revealed that the $VLDLR(1-8)_{HT}$ fragment containing eight CR domains of VLDLR and its subfragments, $VLDLR(1-4)_{HT}$ and $VLDLR(2-4)_{HT}$, interact with $(\beta 15-66)_2$ with practically the same affinity as $sVLDLR_{HT}$ while the affinity of $VLDLR(2-3)_{HT}$ was ~2-fold lower. In contrast, $des(1-8)VLDLR_{HT}$ exhibited no binding. Formation of the complex in solution between the fibrin-binding fragments of VLDLR and $(\beta 15-66)_2$ was detected by fluorescence spectroscopy. In addition, formation of a complex between $VLDLR(2-4)_{HT}$ and $(\beta 15-66)_2$ in solution was confirmed by size-exclusion chromatography. Thus, the results obtained indicate that minimal fibrin-binding structures are located within the second and third CR domains of the VLDL receptor and the presence of the fourth CR domain is required for high-affinity binding. They also indicate that tryptophan residues of CR domains are involved in this binding.

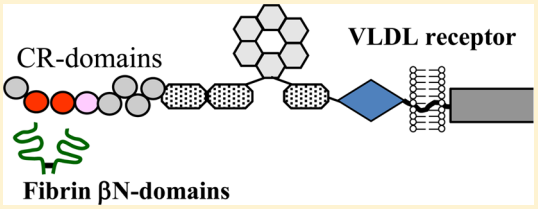

Fibrinogen is a complex multifunctional plasma protein that has been identified as an independent risk factor for cardiovascular diseases. Besides its prominent role in hemostasis, fibrinogen participates in various physiological and pathological processes, including inflammation. Numerous data suggest that fibrin(ogen) plays a prominent role in transendothelial migration of leukocytes, which is a key step in the recruitment of leukocytes from the circulation to sites of inflammation. It was suggested more than two decades ago that binding of fibrinogen to vascular cell receptors mediates a specific pathway of cell-to-cell adhesion by bridging together leukocytes and endothelial cells.[1] Further, it was hypothesized that such bridging occurs through the interaction of fibrinogen with the leukocyte receptor Mac-1 and endothelial cell receptor ICAM-1 and may contribute to leukocyte transmigration.[1,2] Another hypothesis proposed later suggests that fibrin degradation products promote leukocyte transmigration by bridging leukocytes to the endothelium through the interaction with leukocyte integrin CD11c and endothelial cell receptor VE-cadherin.[3,4] We have recently discovered that fibrin interacts with another endothelial cell receptor, very low density lipoprotein receptor (VLDLR), and this interaction also promotes leukocyte transmigration.[5] This discovery suggests a novel fibrin−VLDLR interaction-dependent pathway of leukocyte transmigration in which fibrin−VLDLR interaction plays a key role.

Plasma protein fibrinogen is a chemical dimer consisting of two identical subunits, each of which is formed by three nonidentical polypeptide chains, Aα, Bβ, and γ[6] (Figure 1A). These chains are folded into a number of structural and/or functional domains[7,8] that are involved in multiple fibrin(ogen) interactions. Conversion of fibrinogen into fibrin occurs after thrombin-mediated sequential cleavage of fibrinopeptides A and B from the NH_2-terminal portions of the Aα and Bβ chains, respectively, that are located in the central region of the fibrinogen molecule. Fibrin molecules polymerize spontaneously to form a fibrin clot, which prevents blood loss after vascular injury and serves as a provisional matrix on which different cell types adhere, migrate, and proliferate during the subsequent wound healing process.

In contrast to fibrinogen, which is rather inert in the circulation, polymeric fibrin is highly reactive toward various proteins and cell types because of the exposure and/or activation of its multiple binding sites upon polymer formation. Such reactivity of fibrin provides its participation in various physiological and pathological processes, including wound

Received: May 28, 2015
Published: July 7, 2015

DOI: 10.1021/acs.biochem.5b00582
Biochemistry 2015, 54, 4751−4761

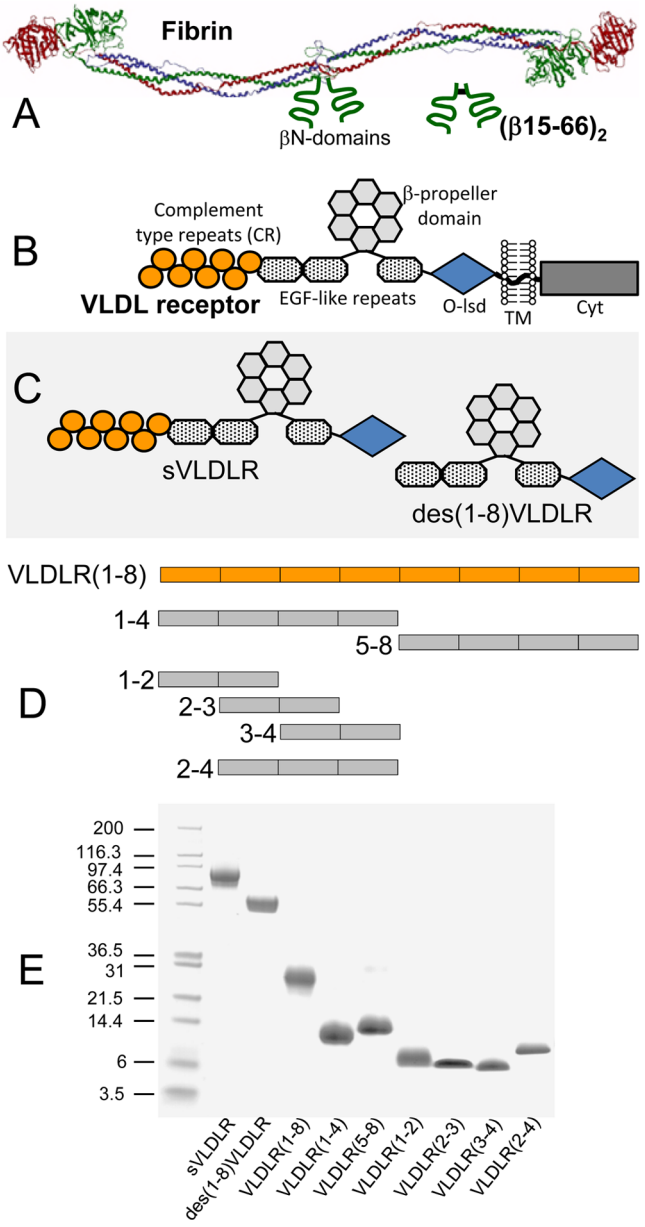

Figure 1. Schematic representation of fibrin, the VLDL receptor, and recombinant fragments prepared for this study. (A) Ribon diagram of a fibrinogen molecule based on its crystal structure.[8] Individual fibrinogen chains Aα, Bβ, and γ are colored blue, green, and red, respectively. The βN domains of fibrin, whose structures have not been identified, are shown schematically as two curved green lines, and the recombinant $(\beta 15-66)_2$ fragment corresponding to these domains is shown on the right. (B) Diagram of the VLDL receptor consisting of CR repeats (domains), EGF-like repeats (domains), the β-propeller domain, the O-linked sugar domain (O-lsd), and transmembrane (TM) and cytoplasmic (Cyt) domains. (C and D) Diagrams of the recombinant $sVLDLR_{HT}$ and $des(1-8)VLDLR_{HT}$ fragments expressed in the Drosophilla Expression System and VLDLR fragments expressed in *Escherichia coli*, respectively. (E) Sodium dodecyl sulfate−polyacrylamide gel electrophoresis analysis of the recombinant VLDLR fragments presented in panels C and D. The left outer lane contains Mark 12 protein markers of the indicated molecular masses.

healing, which at the early stage includes migration of leukocytes to places of injury, i.e., inflammation. Removal of fibrinopeptides B results in the activation of fibrin βN domains, including β chain residues 15−64.[7,9] It was shown that these domains interact with endothelial receptor VE-cadherin,[10] and this interaction promotes fibrin-dependent angiogenesis.[11] It was also shown that fibrin degradation products containing these domains promote leukocyte transmigration and thereby inflammation.[3,4] Our study revealed that interaction of fibrin with the endothelial VLDL receptor also occurs through these domains.[5] Furthermore, we found that the recombinant $(\beta 15-66)_2$ fragment, which mimics the dimeric arrangement of these domains in fibrin, interacts with VE-cadherin and the VLDL receptor with practically the same affinity as fibrin.[5,9,12] Thus, this dimeric fragment preserves functional properties of fibrin βN domains.

The VLDL receptor is a member of the low-density lipoprotein (LDL) receptor family. It is found in different tissues, including vascular endothelium.[13,14] VLDLR consists of a number of extracellular domains that are involved in ligand binding, the transmembrane domain, and the cytoplasmic domain[14,15] (Figure 1B). Originally, VLDLR was proposed to function as a peripheral lipoprotein receptor involved in the delivery of triglyceride-rich lipoproteins to peripheral tissue.[16,17] Later, it was shown that this receptor plays an important role in reelin signaling,[18,19] angiogenesis, and tumor growth.[14,20] Finally, our recent study has revealed a novel function for the VLDL receptor. Namely, we found that this receptor promotes transendothelial migration of leukocytes through interaction with fibrin.[5] We also found that the VLDLR−fibrin interaction occurs with a very high affinity and involves the βN domains of fibrin.[5] Besides these, nothing is known about this novel interaction. The major objectives of this study were to further characterize the interaction between fibrin and the VLDL receptor and localize the fibrin-binding site within the extracellular portion of this receptor.

EXPERIMENTAL PROCEDURES

Proteins, Peptides, and Reagents. The recombinant $(B\beta 1-66)_2$ fragment was produced in *Escherichia coli* and purified as previously described.[9] This fragment was treated with thrombin to produce a fibrin-related $(\beta 15-66)_2$ fragment using the previously described procedure.[21] Human recombinant receptor-associated protein (RAP) was expressed in *E. coli* and purified as previously described.[22] Mouse anti-hVLDLR monoclonal antibodies 1H5, 5F3, and 1H10[23] were kindly provided by D. Strickland (University of Maryland, Baltimore, MD). The anti-His(C-term) antibody (anti-His tag mAb) conjugated with HRP was from Invitrogen (Carlsbad, CA). Goat secondary anti-mouse polyclonal antibodies conjugated with HRP and HRP substrate SureBlue TMB were from KPL (Gaithersburg, MD). Cyanogen bromide-activated Sepharose 4B and Thrombin CleanCleave kit were obtained from Sigma (St. Louis, MO).

Preparation of Recombinant VLDLR Fragments in the *Drosophila* Expression System. The soluble form of human VLDL receptor, $sVLDLR_{HT}$, which contains the entire extracellular portion of the receptor, including amino acid residues 1−770, and its fragment $des(1-8)VLDLR_{HT}$ lacking eight CR repeats (residues 329−770), both tagged with six His residues (His-tag) at the C-termini, were prepared using the *Drosophila* Expression System (Invitrogen). The expression and purification of these fragments were performed utilizing previously described protocols[23−25] with some modifications. Namely, the cDNAs encoding both fragments were amplified by polymerase chain reaction (PCR) using a plasmid carrying the full-length human VLDLR sequence. The following

DOI: 10.1021/acs.biochem.5b00582
Biochemistry 2015, 54, 4751−4761

Table 1. Primers Used To Produce Recombinant VLDLR Fragments

fragment	sequence	number of primers used	
		forward	reverse
$VLDLR(1-8)_{HT}$	$Gly^{1}-Cys^{328}(His)_6$	1	2
$VLDLR(1-4)_{HT}$	$Gly^{1}-Pro^{163}(His)_6$	1	3
$VLDLR(5-8)_{HT}$	$Pro^{164}-Cys^{328}(His)_6$	4	2
$VLDLR(1-2)_{HT}$	$Gly^{1}-His^{82}(His)_6$	1	5
$VLDLR(2-3)_{HT}$	$Lys^{42}-Asn^{124}(His)_6$	6	7
$VLDLR(3-4)_{HT}$	$Arg^{84}-Pro^{163}(His)_6$	8	3
$VLDLR(2-4)_{HT}$	$Lys^{42}-Pro^{163}(His)_6$	6	3
primer number	primer sequence[a]		
1	5′-TGGCGCCTCATATGGGGAGAAAAGCCAAATGTGAACCC-3′		
2	5′-GCTGCTCGAG**TCA**GTGGTGGTGGTGGTGGTGACACTCTTTCAGGGGCTCATC-3′		
3	5′-TTTAAACTCGAG**TCA**GTGGTGGTGGTGGTGGTGCGGGGCACAGTCCAGCTC-3′		
4	5′-GATCGCCAACATATGCCAACCTGTGGCGCCCATG-3′		
5	5′-GCTGCTCGAG**TCA**GTGGTGGTGGTGGTGGTGGCACTGTTCTGGGCTTTC-3′		
6	5′-TGGCGCCTCATATGAAGACGTGTGCTGAATCTGACTTCG-3′		
7	5′-TTTAAACTCGAG**TCA**GTGGTGGTGGTGGTGGTGATTGCCACAGTTTTCTTC- 3′		
8	5′-TGGCGCCTCATATGAGAACATGCCGCATACATG-3′		

[a]Restrictase−recognition sequences are underlined; stop codons are shown in bold.

oligonucleotides were used as primers in which restrictase−recognition sites are underlined and the stop codon is shown in bold: 5′-GGCGGCCGCTCGGGGGGGAGAAAAGCCAAATG-3′ (forward primer for $sVLDLR_{HT}$), 5′-GGCGGCCGCTCGGGCATATAAACGAATGCTTG-3′ [forward primer for $des(1-8)VLDLR_{HT}$], and 5′-CCGCGCCCGTTTAAACT**CA**ATGGTGATGGTGATGATGAGAAGTCCCTTTTGGGGG-3′ (reverse primer for both fragments). The PCR products were subcloned into the pMT/BiP/V5-HisC vector for secreted expression in *Drosophila melanogaster* Schneider 2 (S2) cells using *Ava*I and *Pme*I restriction sites and then transformed into DH5α *E. coli* host cells (Invitrogen). All resultant clones were sequenced to confirm the integrity of the coding sequences. S2 cells were cotransfected with the expression plasmids encoding the fragments and pCoBlas vector, and stable transfectants resistant to blasticidin were selected. For large-scale expression, stable S2 cells were grown in shaker flasks at 28 °C in *Drosophila* serum-free medium (HyClone SFX) supplemented with 20 mM L-glutamine, penicillin/streptomycin, Fungizone, and blasticidin at 25 μg/mL (Invitrogen). Expression of the fragments was induced by adding 0.5 mM $CuSO_4$, and conditioned medium was collected on day 5 of induction. The amount of the fragments in the conditioned serum free medium (HyClone SFX) was determined by Western blot analysis with the anti-His(C-term) antibody conjugated with HRP. Both $sVLDLR_{HT}$ and $des(1-8)VLDLR_{HT}$ fragments were purified from conditioned media, depleted of Cu^{2+} with chelating resin Chelex 100 (Bio-Rad, Hercules, CA), using affinity chromatography on Talon Metal Affinity Resin (Clontech Laboratories, Mountain View, CA), and further purified by size-exclusion chromatography on Superdex 200 (GE Healthcare, Piscataway, NJ).

Preparation of Recombinant VLDLR Fragments in the *E. coli* Expression System. Recombinant VLDLR fragments, $VLDLR(1-8)_{HT}$, $VLDLR(1-4)_{HT}$, $VLDLR(5-8)_{HT}$, $VLDLR(1-2)_{HT}$, $VLDLR(2-3)_{HT}$, $VLDLR(3-4)_{HT}$, and $VLDLR(2-4)_{HT}$, including amino acid residues 1−328, 1−163, 164−328, 1−82, 42−124, 84−163, and 42−163, respectively, were produced in *E. coli* strain BL21(DE3)pLysS using the pET-20b expression vector (Novagen). All fragments were tagged with six His residues. The cDNA fragments encoding these regions were produced by PCR using as a template the full-length cDNA encoding human VLDLR; the primers are listed in Table 1. The PCR products were subcloned into the pET20b expression vector using *Nde*I and *Xho*I restriction sites and then transformed into DH5α *E. coli* host cells (Invitrogen). All resulting clones were sequenced to confirm the integrity of the coding sequences. For the preparation of the recombinant fragments, the BL21(DE3)-pLysS *E. coli* host cells were transformed with the resulting plasmids and all fragments were produced and refolded following the procedures described previously.[26] The refolded fragments were purified by size-exclusion chromatography on Superdex 200 followed by affinity chromatography on RAP-Sepharose. The purity of all fragments was verified by sodium dodecyl sulfate−polyacrylamide gel electrophoresis (Figure 1E).

Preparation of the Recombinant $VLDLR(1-8)_{HT}$ Fragment Mutant. The Trp105Ala mutant of the $VLDLR(1-8)_{HT}$ fragment was produced by site-directed mutagenesis using the QuikChange Multi Site-Directed Mutagenesis kit (Stratagene, La Jolla, CA). The pET-20b construct containing DNA encoding the VLDLR(1−328) fragment tagged with six His residues was modified by using the mutagenic primer 5′-TCAGTGTATCCCAGTGTCCGCGAGATGTGATGGTGAAAAT-3′. The mutation was confirmed by sequencing throughout the entire VLDLR1−328 coding region of the mutant plasmid. The mutant fragment was produced in *E. coli* strain BL21(DE3)pLysS and refolded and purified by the procedures described above for the wild-type $VLDLR(1-8)_{HT}$ fragment.

Protein Concentration Determination. Concentrations of the expressed VLDLR fragments were determined spectrophotometrically using theoretical extinction coefficients ($E_{280,1\%}$) estimated from fragments' sequences by the ProtParam online tool (http://www.expasy.ch/tools/protparam.html). Molecular masses of these fragments were also estimated using ProtParam. The following molecular masses and $E_{280,1\%}$ values were obtained: $sVLDLR_{HT}$, 85.6 kDa and 12.9; $des(1-8)VLDLR_{HT}$, 49.7 kDa and 15.0; $VLDLR(1-8)_{HT}$, 36.8 kDa and 9.8; $VLDLR(1-4)_{HT}$, 18.7 kDa and 9.7; $VLDLR(5-8)_{HT}$, 19.0 kDa and 9.5; $VLDLR(1-2)_{HT}$, 9.9 kDa

DOI: 10.1021/acs.biochem.5b00582
Biochemistry 2015, 54, 4751−4761

and 11.9; VLDLR(2−3)$_{HT}$, 9.9 kDa and 11.9; VLDLR(3−4)$_{HT}$, 9.5 kDa and 6.6; VLDLR(2−4)$_{HT}$, 14.0 kDa and 8.7. The concentration of the (β15−66)$_2$ fragment was determined as previously described.[9]

Fluorescence Spectroscopy. Fluorescence spectra were recorded in an SLM 8000-C fluorometer. Fluorescence measurements of thermal unfolding were performed by monitoring the ratio of the intensity at 370 nm to that at 330 nm with excitation at 280 nm in the same fluorometer. The temperature was controlled with a circulating water bath. Protein/fragment concentrations were 0.02−0.04 mg/mL. All experiments were performed in a 1 cm path-length quartz cuvette in 20 mM Tris buffer (pH 7.4) and 150 mM NaCl (TBS) containing 1 mM $CaCl_2$.

Size-Exclusion Chromatography. Analytical size-exclusion chromatography was used to analyze formation of a complex between the (β15−66)$_2$ and VLDLR(2−4)$_{HT}$ fragments. The experiments were performed with a fast protein liquid chromatography system (FPLC, Pharmacia) on a Superdex 75 column at a flow rate of 0.5 mL/min. Typically, 500 μL of individual fragments or their mixture was loaded onto the column equilibrated with TBS containing 1 mM Ca^{2+} followed by elution with the same buffer. Protein elution was monitored by measuring the absorbance at 280 nm.

Solid-Phase Binding Assay. Wells of Immulon 2HB microtiter plates were coated overnight with the (β15−66)$_2$ fragment at 2 μg/mL in 0.1 M Na_2CO_3 (pH 9.5) (coating buffer) at 4 °C. The wells were then blocked with Blocker BSA in TBS (Thermo Scientific, Rockford, IL) for 1 h at room temperature. Following washing with TBS containing 0.05% Tween 20 and 1 mM $CaCl_2$ (ELISA binding buffer), the indicated concentrations of VLDLR fragments in this buffer were added to the wells and also to control wells coated just with Blocker BSA in TBS and incubated for 1 h at 37 °C. Bound fragments were detected by reaction with the anti-His monoclonal antibody conjugated with HRP (1 h at 37 °C). Alternatively, bound VLDLR fragments were detected by reaction with a mixture of anti-VLDLR mAb 1H5, 5F3, and 1H10 (1 h at 37 °C) and the HRP-conjugated donkey anti-mouse polyclonal antibodies (1 h at 37 °C). The peroxidase substrate, SureBlue TMB (KPL, Gaithersburg, MD), was added to the wells, and the amount of bound ligand was measured spectrophotometrically at 450 nm. Data were analyzed by nonlinear regression analysis using eq 1:

$$A = A_{max}/(1 + K_d/[L]) \quad (1)$$

where A represents the absorbance of the oxidized substrate, which is assumed to be proportional to the amount of ligand bound, A_{max} is the absorbance at saturation, [L] is the molar concentration of the ligand, and K_d is the equilibrium dissociation constant.

Surface Plasmon Resonance Analysis. Interaction of the (β15−66)$_2$ fragment with VLDLR fragments was studied by surface plasmon resonance (SPR) using the BIAcore 3000 biosensor (GE Healthcare), which measures the association and dissociation of proteins in real time. Immobilization of VLDLR fragments to the activated surface of CM5 sensor chip was performed using the amine coupling kit (GE Healthcare), as specified by the manufacturer. Binding experiments were performed in HBS-P [10 mM HEPES buffer (pH 7.4), 150 mM NaCl, and 0.005% Surfactant P20] containing 1 mM $CaCl_2$ at a flow rate of 20 μL/min. The (β15−66)$_2$ fragment was injected at increasing concentrations, and the association/dissociation between it and immobilized VLDLR fragments was monitored as the change in the SPR response. To regenerate the chip surface, complete dissociation of the complex was achieved by adding 100 mM H_3PO_4 for 30 s followed by re-equilibration with binding buffer. Experimental data were analyzed using BIAevaluation version 4.1 supplied with the instrument. The equilibrium dissociation constant, K_d, was calculated with the equation $K_d = k_{diss}/k_{ass}$, where k_{ass} and k_{diss} represent kinetic constants that were estimated by global analysis of the association and dissociation data, respectively, using the 1:1 Langmurian interaction model (kinetic analysis). To confirm the kinetic analysis, K_d was also estimated by analysis of the association data using the steady-state affinity model (equilibrium analysis).

RESULTS

Preparation and Characterization of the Extracellular Portion of the VLDL Receptor and Its Fragments. The extracellular portion of the VLDL receptor is composed of eight complement-type repeats (CR repeats or domains), three EGF-like domains, the β-propeller, and O-linked sugar domains (Figure 1B). Among these domains, CR domains (~42 residues each) compose the ligand-binding region[27] and are the most probable candidates for binding to fibrin. To test this suggestion, we prepared a soluble extracellular portion of the VLDL receptor (sVLDLR$_{HT}$) and its subfragments, VLDLR(1−8)$_{HT}$ and des(1−8)VLDLR$_{HT}$, containing all eight CR domains and the rest of the extracellular portion, respectively (Figure 1C,D).

The sVLDLR$_{HT}$ and des(1−8)VLDLR$_{HT}$ fragments, tagged with six His residues at the C-termini to facilitate their purification and detection, were prepared using the *Drosophila* expression system. To test the folding status of these fragments, we used fluorescence spectroscopy. At 4 °C, the sVLDLR$_{HT}$ and des(1−8)VLDLR$_{HT}$ fragments exhibited fluorescence spectra with maxima at 343 and 338 nm, respectively (Figure 2A, left and right insets, and Table 2), indicating that they both contain compact structures. When the fragments were heated in the fluorometer while the ratio of fluorescence intensity at 370 nm to that at 330 nm was monitored as the measure of the spectral shift that accompanies unfolding, both fragments exhibited a sigmoidal denaturation transition with a midpoint (T_m) at ~63 °C (Figure 2A), further confirming that they are folded into compact structures. It should be noted that at 90 °C the maxima of sVLDLR$_{HT}$ and des(1−8)VLDLR$_{HT}$ spectra (λ_{max}) were shifted to 347 and 345 nm, respectively (Figure 2A, left and right insets, and Table 2), suggesting that upon heat-induced denaturation some of their Trp residues were only partially exposed.

Our attempts to express the His-tagged VLDLR(1−8) fragment in the *Drosophila* expression system were not successful. Although immunoblot analysis revealed the presence of this fragment in the cells, no such fragment in the medium was detected, most probably because of poor or no secretion to the medium. Therefore, we expressed this fragment in the *E. coli* expression system that was previously used for preparation of the GST−VLDLR(1−8) fusion protein.[26] Because this fragment contains multiple disulfide bonds, it was refolded and purified using protocols described in Experimental Procedures. The heat denaturation study of the VLDLR(1−8)$_{HT}$ fragment revealed no well-expressed sigmoidal transition (Figure 2B). However, the spectral shift from 349 to 352 nm upon heating this fragment from 4 to 90 °C (Figure 2B, left inset, and Table

DOI: 10.1021/acs.biochem.5b00582
Biochemistry 2015, 54, 4751−4761

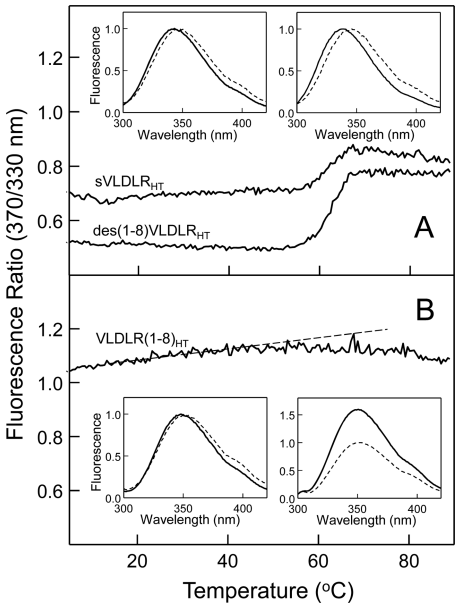

Figure 2. Fluorescence-detected thermal unfolding of the extracellular portion of the VLDL receptor (sVLDLR$_{HT}$) and its subfragments, des(1−8)VLDLR$_{HT}$ and VLDLR(1−8)$_{HT}$. (A) Melting curves obtained upon heating of the sVLDLR$_{HT}$ and des(1−8)VLDLR$_{HT}$ fragments. Fluorescence spectra of sVLDLR$_{HT}$ and des(1−8)-VLDLR$_{HT}$ at 4 °C (—) and 90 °C (---) are shown in the left and right insets, respectively. All experiments were performed in TBS containing 1 mM $CaCl_2$. (B) Melting curve obtained upon heating of the VLDLR(1−8)$_{HT}$ fragment. The dashed line represents linear extrapolation of fluorescence ratio values to highlight a downturn of this parameter. Fluorescence spectra of VLDLR(1−8)$_{HT}$ at 4 °C (—) and 90 °C (---) are shown in the left inset; fluorescence spectra of VLDLR(1−8)$_{HT}$ in the presence of 1 mM $CaCl_2$ (—) and 0.5 mM EDTA (---) are shown in the right inset.

2) and the downward change in fluorescence ratio, which starts at approximately the same temperature as denaturation of sVLDLR$_{HT}$ and des(1−8)VLDLR$_{HT}$ and may reflect aggregation upon denaturation, suggest that this fragment is folded into a compact structure. Because it was shown that properly folded CR domains of the LDL receptor bind Ca^{2+} and this binding results in a significant increase in the fluorescence intensity of their Trp residues,[28] we next tested the effect of Ca^{2+} on the fluorescence intensity of the VLDLR(1−8)$_{HT}$ fragment. The experiments revealed an ∼80% increase in the fluorescence intensity of VLDLR(1−8)$_{HT}$ upon addition of 1 mM Ca^{2+} (Figure 2B, right inset). No such increase upon addition of Ca^{2+} was observed in the presence of 4 M GdmCl and 1 mM DTT, which were added to denature the VLDLR(1−8)$_{HT}$ fragment (not shown). Altogether, these results clearly indicate that VLDLR(1−8)$_{HT}$ was properly folded. It should be noted that the final yield of the properly folded His-tagged VLDLR(1−8)$_{HT}$ fragment was ∼10-fold higher than that of VLDLR(1−8) prepared from the GST−VLDLR(1−8) fusion protein using previously described protocols.[26]

Localization of the Fibrin-Binding Site in the CR Domain Region of the VLDL Receptor. Our previous study revealed that the VLDL receptor interacts with fibrin exclusively through the βN domains.[5] Furthermore, this study also revealed that the $(\beta15-66)_2$ fragment, which mimics the dimeric arrangement of these domains in fibrin (Figure 1A), exhibits practically the same affinity for sVLDLR as fibrin[5] but, in contrast to the latter, is highly soluble. Therefore, in the study presented here, we used the $(\beta15-66)_2$ fragment as the simplest soluble mimetic of fibrin. In an ELISA, sVLDLR$_{HT}$ and VLDLR(1−8)$_{HT}$ both bound to immobilized $(\beta15-66)_2$ while the des(1−8)VLDLR$_{HT}$ fragment exhibited no binding (Figure 3A). This finding was confirmed by SPR experiments (Figure 3B). The observed binding occurred in the presence of 1 mM Ca^{2+}; when the experiments were performed in the presence of 100 mM EDTA, practically no binding was detected (Figure 3A, inset). Altogether, these results indicate that the fibrin−VLDLR interaction is Ca^{2+}-dependent, the fibrin-binding site is located within eight CR domains of the VLDL receptor, and the remaining extracellular domains of this receptor are not involved in fibrin binding.

It should be noted that in ELISA experiments, in which bound sVLDLR$_{HT}$ and sVLDLR(1−8)$_{HT}$ were detected using the anti-His tag monoclonal antibody (mAb), the affinities of their binding to the $(\beta15-66)_2$ fragment were very similar [K_d values of 16.4 and 16.3 nM, respectively (Table 3)], further confirming that sVLDLR(1−8)$_{HT}$ is properly folded. At the same time, these affinities were lower than the affinity we determined earlier for the interaction of non-His tagged sVLDLR with fibrin and $(\beta15-66)_2$ using a mixture of anti-VLDLR(1−8) mAbs [K_d = 5.7 nM (Table 3)]. To clarify the reason for such a discrepancy, we performed ELISA experiments in which bound His-tagged sVLDLR$_{HT}$ and VLDLR(1−8)$_{HT}$ fragments were detected with the same mixture of mAbs. The experiments revealed that the affinities of interaction of

Table 2. Fluorescence Parameters for Denaturation of the VLDLR Fragments and Their Interaction with Ca^{2+}, RAP, and the $(\beta15-66)_2$ Fragment

	denaturation[a]	with Ca^{2+}	with Ca^{2+} (denatured[b])	with RAP	with+ $(\beta15-66)_2$
VLDLR fragment	λ_{max} shift (nm)	I_0 increase (%)	I_0 increase (%)	λ_{max} shift (nm)	λ_{max} shift (nm)
sVLDLR$_{HT}$	343 → 347	–	–	–	–
VLDLR(1−8)$_{HT}$	349 → 352	80	no	349 → 347	349 → 347
des(1−8)VLDLR$_{HT}$	338 → 345	–	–	–	–
VLDLR(1−4)$_{HT}$	351 → 354[c]	75	no	351 → 347	351 → 348
VLDLR(5−8)$_{HT}$	351 → 354	60	no	351 → 351	351 → 351
VLDLR(1−2)$_{HT}$	351 → 353[c]	89	no	351 → 351	351 → 351
VLDLR(2−3)$_{HT}$	352 → 352	142	no	352 → 346	352 → 349
VLDLR(3−4)$_{HT}$	353 → 353	122	no	353 → 353	353 → 353
VLDLR(2−4)$_{HT}$	353 → 353	236	no	353 → 347	353 → 348

[a]Denaturation was performed by heating to 90 °C. [b]Denaturation was performed by addition of 4 M GdmCl and 1 mM DTT. [c]Denaturation was performed by heating to 90 °C in the presence of 4 M urea.

DOI: 10.1021/acs.biochem.5b00582
Biochemistry 2015, 54, 4751−4761

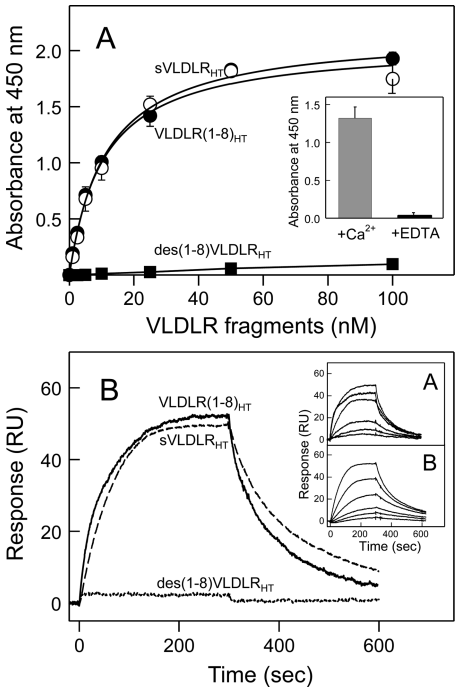

Figure 3. Analysis of interaction of the sVLDLR$_{HT}$, des(1−8)VLDLR$_{HT}$, and VLDLR(1−8)$_{HT}$ fragments with the $(\beta 15-66)_2$ fragment. (A) ELISA-detected interaction between the $(\beta 15-66)_2$ and VLDLR fragments. Increasing concentrations of sVLDLR$_{HT}$ (●), VLDLR(1−8)$_{HT}$ (○), or des(1−8)VLDLR$_{HT}$ (■) were incubated with microtiter wells coated with $(\beta 15-66)_2$, and the bound fragments were detected with anti-His tag mAb, as described in Experimental Procedures. The curves for sVLDLR$_{HT}$ and VLDLR(1−8)$_{HT}$ represent the best fit of the data to eq 1, and the determined K_d values are listed in Table 3; error bars represent the standard deviation of triplicate determinations. Binding of sVLDLR$_{HT}$ at 10 nM in the presence of 1 mM Ca^{2+} or 100 mM EDTA is shown in the inset. All experiments were performed in ELISA binding buffer. (B) SPR-detected interaction between the $(\beta 15-66)_2$ and VLDLR fragments. The $(\beta 15-66)_2$ fragment at 10 or 100 nM in HBS-P buffer with 1 mM $CaCl_2$ was added to immobilized sVLDLR$_{HT}$ (---), VLDLR(1−8)$_{HT}$ (—), or des(1−8)VLDLR$_{HT}$ (···), and its association/dissociation was monitored in real time by registering the resonance signal (response). The insets show analysis of interaction of $(\beta 15-66)_2$ with sVLDLR$_{HT}$ (inset A) or VLDLR(1−8)$_{HT}$ (inset B) by SPR. $(\beta 15-66)_2$ at increasing concentrations, 0.25, 0.5, 1, 2.5, 5, and 10 nM, was added to the immobilized VLDLR fragments, and its association/dissociation was monitored in real time.

these fragments with $(\beta 15-66)_2$ are higher than those determined with anti-His mAb and are very close to the affinity determined earlier for non-His-tagged sVLDLR (Table 3). Furthermore, the values of equilibrium dissociation constants determined by SPR turned out to be very similar to those determined in these ELISA experiments (Figure 3B, insets, and Table 3). These results suggest that His tag may be partially unavailable in the sVLDLR$_{HT}$ and VLDLR(1−8)$_{HT}$ fragments and that K_d values determined by SPR are more reliable than those determined by an ELISA using anti-His tag mAb. They also indicate that His-tagged VLDLR(1−8)$_{HT}$ expressed in *E. coli* after refolding and purification adopts a physiologically active conformation similar to that of sVLDLR and His-tagged sVLDLR$_{HT}$ prepared using the *Drosophila* expression system.

Further Localization of the Fibrin-Binding Site in the VLDL Receptor. To further localize the fibrin-binding site within the CR domains of the VLDL receptor, we first prepared two fragments, VLDLR(1−4)$_{HT}$ and VLDLR(5−8)$_{HT}$, including CR domains 1−4 and 5−8, respectively, both containing a His tag at their C-termini (Figure 1D). As in the case with the VLDLR(1−8)$_{HT}$ fragment, our attempts to express these fragments in the *Drosophila* expression system were not successful, most probably for the same reason mentioned above for VLDLR(1−8)$_{HT}$. Therefore, we expressed them in the *E. coli* expression system and refolded them using the same refolding protocol that was used for VLDLR(1−8)$_{HT}$. After refolding, both fragments were fractionated on a Superdex-75 column to separate their monomeric fractions, and the folding status of these fractions was tested by fluorescence spectroscopy. At 4 °C, the VLDLR(5−8)$_{HT}$ fragment exhibited a fluorescence spectrum with a λ_{max} at 351 nm, while at 90 °C, the maximum was shifted to 354 nm (Table 2), confirming that this fragment is folded into a compact structure. The VLDLR(1−4)$_{HT}$ fragment also exhibited a spectrum with a λ_{max} at 351 nm that was practically unchanged upon heating to 90 °C (not shown). However, the maximum was shifted to 354 nm upon heating to 90 °C in the presence of 4 M urea (Table 2), indicating that this fragment is also folded into a compact structure, which is more thermostable than that of VLDLR(5−8)$_{HT}$. In addition, both fragments exhibited a significant increase in fluorescence intensity upon addition of Ca^{2+} while no such increase was observed upon addition of Ca^{2+} in the presence of denaturing agents, 4 M GdmCl and 1 mM DTT (Table 2), further confirming that they are properly folded.

Table 3. Equilibrium Dissociation Constants (K_d) for the Interaction of the VLDLR Fragments with the $(\beta 15-66)_2$ Fragment

VLDLR fragment	K_d (nM) ELISA[a]	K_d (nM) ELISA[b]	K_d (nM) SPR	binding to RAP-Sepharose
sVLDLR	–	5.7 ± 0.4[c]	3.6 ± 0.9[c]	yes
sVLDLR$_{HT}$	16.4 ± 6.4	2.5 ± 1.2	3.6 ± 0.2	yes
VLDLR(1−8)$_{HT}$	16.3 ± 7.8	3.4 ± 1.5	3.1 ± 1.1	yes
des(1−8)VLDLR$_{HT}$	nb[d]	–	nb[d]	nb[d]
VLDLR(1−4)$_{HT}$	60 ± 16	–	3.7 ± 0.1	yes
VLDLR(5−8)$_{HT}$	nb[d]	–	nb[d]	nb[d]
VLDLR(1−2)$_{HT}$	nb[d]	–	nb[d]	nb[d]
VLDLR(2−3)$_{HT}$	78 ± 8	–	9.5 ± 0.4	yes
VLDLR(3−4)$_{HT}$	nb[d]	–	nb[d]	nb[d]
VLDLR(2−4)$_{HT}$	40 ± 2	–	4.6 ± 0.1	yes

[a]Determined using anti-His tag mAb (see the text). [b]Determined using anti-VLDLR(1−8) mAbs (see the text). [c]Determined previously.[5] [d]No binding.

DOI: 10.1021/acs.biochem.5b00582
Biochemistry 2015, 54, 4751−4761

In ELISA experiments, the VLDLR(1−4)$_{HT}$ fragment exhibited binding to immobilized (β15−66)$_2$ while VLDLR(5−8)$_{HT}$ failed to bind (Figure 4A). This finding was

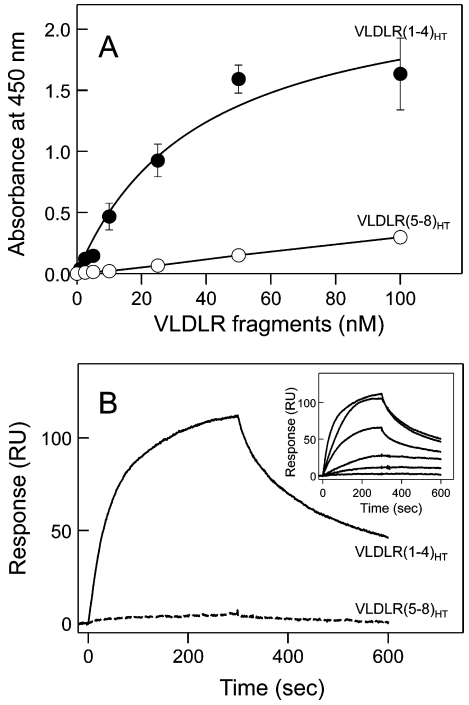

Figure 4. Analysis of interaction of the VLDLR(1−4)$_{HT}$ and VLDLR(5−8)$_{HT}$ fragments with the (β15−66)$_2$ fragment. (A) ELISA-detected interaction between the (β15−66)$_2$ and VLDLR fragments. Increasing concentrations of VLDLR(1−4)$_{HT}$ (●) or VLDLR(5−8)$_{HT}$ (○) were incubated with microtiter wells coated with (β15−66)$_2$, and the bound fragments were detected with anti-His tag mAb, as described in Experimental Procedures. The curve for VLDLR(1−4)$_{HT}$ represents the best fit of the data to eq 1, and the determined K_d value is presented in Table 3; error bars represent the standard deviation of triplicate determinations. All experiments were performed in ELISA binding buffer. (B) SPR-detected interaction between the (β15−66)$_2$ and VLDLR fragments. The (β15−66)$_2$ fragment at 10 or 100 nM in HBS-P buffer with 1 mM $CaCl_2$ was added to the immobilized VLDLR(1−4)$_{HT}$ (—) or VLDLR(5−8)$_{HT}$ (---) fragment, respectively, and its association/dissociation was monitored in real time. The insets show analysis of interaction of the (β15−66)$_2$ fragment with VLDLR(1−4)$_{HT}$ by SPR. (β15−66)$_2$ at increasing concentrations, 0.25, 0.5, 1, 2.5, 5, and 10 nM, was added to immobilized VLDLR(1−4)$_{HT}$, and its association/dissociation was monitored in real time.

confirmed in SPR experiments (Figure 4B). These results indicate that the fibrin-binding site is located within the first four CR domains of the VLDL receptor. The value of K_d for the interaction of VLDLR(1−4)$_{HT}$ with (β15−66)$_2$ determined by an ELISA using for detection anti-His tag mAb was found to be 60 nM, ∼4-fold higher than that determined for sVLDLR$_{HT}$ and VLDLR(1−8)$_{HT}$. However, a K_d value of 3.7 nM determined for this interaction by SPR, which provides a more reliable estimate of K_d as mentioned above, was practically the same as those for sVLDLR$_{HT}$ and VLDLR(1−8)$_{HT}$ (Table 3). This indicates that the VLDLR(1−4)$_{HT}$ fragment preserves the physiologically active conformation of the corresponding region of the VLDL receptor.

To test which of the first four CR domains of VLDLR are involved in binding of fibrin, we next expressed three overlapping fragments, VLDLR(1−2)$_{HT}$, VLDLR(2−3)$_{HT}$, and VLDLR(3−4)$_{HT}$, containing CR domains 1 and 2, 2 and 3, and 3 and 4, respectively (Figure 1D), in the *E. coli* expression system. Again, as in the case with the other fragments described above, the folding status of each of these fragments was tested by fluorescence spectroscopy. At 4 °C, these fragments exhibited fluorescence spectra with λ_{max} values at 351−353 nm whose positions did not change upon heating to 90 °C (Table 2). However, upon addition of Ca^{2+}, the fluorescence intensity of all three fragments significantly increased and such an increase was not observed when these fragments were under denaturing conditions (Table 2). In addition, the λ_{max} of the VLDLR(1−2)$_{HT}$ spectrum shifted from 351 to 353 nm when this fragment was heated in the presence of 4 M urea, a situation similar to that observed with the VLDLR(1−4)$_{HT}$ fragment. Altogether, these results confirmed that all three fragments were properly folded.

In ELISA experiments, in which bound fragments were detected with anti-His tag mAb, only the VLDLR(2−3)$_{HT}$ fragment bound to immobilized (β15−66)$_2$ while VLDLR(1−2)$_{HT}$ and VLDLR(3−4)$_{HT}$ failed to bind (Table 3). The K_d value determined for this binding was found to be 78 nM, i.e., much higher than those determined for larger VLDLR fragments. However, SPR experiments revealed that this binding occurs with a much higher affinity. Namely, the K_d value determined by SPR was found to be 9.5 nM (Figure 5A

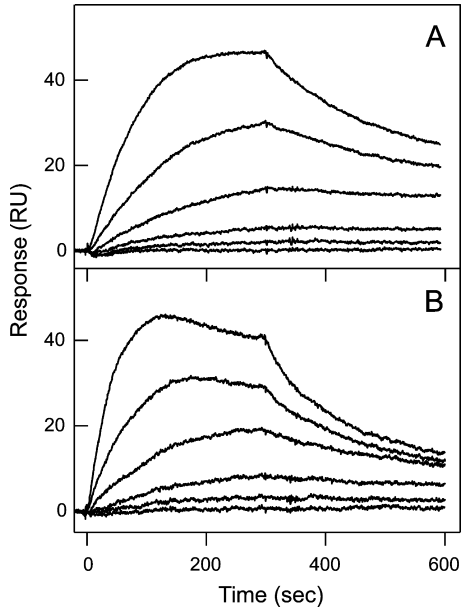

Figure 5. Analysis of interaction of the (β15−66)$_2$ fragment with the (A) VLDLR(2−3)$_{HT}$ and (B) VLDLR(2−4)$_{HT}$ fragments by surface plasmon resonance. (β15−66)$_2$ at increasing concentrations, 0.25, 0.5, 1.0, 2.5, 5.0, and 10 nM, was added to the immobilized VLDLR fragments, and its association/dissociation was monitored in real time. All experiments were performed in HBS-P buffer containing 1 mM $CaCl_2$.

and Table 3), i.e., only ∼2.6-fold higher than that determined by this technique for the interaction of sVLDLR$_{HT}$, VLDLR(1−8)$_{HT}$, and VLDLR(1−4)$_{HT}$ with (β15−66)$_2$. Altogether, these results indicate that a pair of domains, CR domains 2 and 3, is the minimal structure composing the fibrin-binding site.

Because the results described above revealed that the affinity of VLDLR(2−3)$_{HT}$ for (β15−66)$_2$ is lower than that of

DOI: 10.1021/acs.biochem.5b00582
Biochemistry 2015, 54, 4751−4761

VLDLR(1−4)$_{HT}$, this finding raised a question about the possible involvement of neighboring domain(s) in the formation of the high-affinity fibrin-binding site. To address this question, we prepared a recombinant VLDLR(2−4)$_{HT}$ fragment containing CR domains 2−4 (Figure 1D) and confirmed its proper folding by the procedures described above for other recombinant fragments expressed in the *E. coli* expression system. In ELISA and SPR experiments, the VLDLR(2−4)$_{HT}$ fragment interacted with (β15−66)$_2$ and the affinity of its interaction determined by SPR (K_d = 4.6 nM) was higher than that of VLDLR(2−3)$_{HT}$ and comparable with that of VLDLR(1−8)$_{HT}$ and VLDLR(1−4)$_{HT}$ (Figure 5B and Table 3). These results indicate that the presence of the fourth CR domain increases the affinity of CR domains 2 and 3 to fibrin by ∼2-fold. This finding suggests that the fourth CR domain may contribute to the formation of the high-affinity fibrin-binding site in the VLDL receptor.

Fluorescence-Detected Interaction of VLDLR Fragments with (β15−66)$_2$ and RAP. Receptor-associated protein (RAP) is known to be an antagonist of ligand binding of some LDL receptor family members, including VLDLR to which it binds with high affinity.[29] As mentioned in Experimental Procedures, after refolding, all recombinant VLDLR fragments were subjected to size-exclusion chromatography to separate monomeric fractions and then passed through a RAP-Sepharose column. Our subsequent experiments revealed that only those fragments that bound to RAP-Sepharose interacted with (β15−66)$_2$ (Table 3). This is in agreement with our previous finding that RAP inhibits interaction of fibrin and (β15−66)$_2$ with the VLDL receptor.[5] Because interaction of some CR domain-containing fragments with their ligands or RAP was shown to be accompanied by a short-wave shift of their fluorescence spectra,[28,30] we used fluorescence spectroscopy to detect interaction of recombinant VLDLR fragments with (β15−66)$_2$ and RAP in solution.

In a typical experiment, fluorescence spectra of a VLDLR fragment at 1 μM were recorded before and after addition of RAP or (β15−66)$_2$ to a final molar ratio of 1:1 or 1:10, respectively. Figure 6 shows a representative example of short-wave spectral shifts upon addition of RAP or (β15−66)$_2$ to the VLDLR(2−4)$_{HT}$ fragment; the shifts for the remaining fragments are listed in Table 2. The observed spectral shifts of VLDLR(1−8)$_{HT}$ upon addition of RAP or (β15−66)$_2$ were ∼2 nm only, most probably because of the presence of Trp residues that do not participate in the formation of the RAP-binding or fibrin-binding sites. At the same time, the spectral shifts for smaller fragments, VLDLR(1−4)$_{HT}$, VLDLR(2−3)$_{HT}$, and VLDLR(2−4)$_{HT}$, upon addition of RAP or (β15−66)$_2$ were found to be more significant, 4−6 or 3−5 nm, respectively. No such shifts were detected for those fragments that exhibited no interaction with the (β15−66)$_2$ fragment and did not bind to RAP-Sepharose. Altogether, these experiments revealed a short-wave shift in fluorescence spectra of all VLDLR fragments that exhibited affinity for RAP and (β15−66)$_2$, indicating formation of a complex between these fragments and RAP or (β15−66)$_2$ in solution.

Formation of the Complex between VLDLR(2−4)$_{HT}$ and (β15−66)$_2$ Detected by Size-Exclusion Chromatography. To further test the interaction of VLDLR fragments with the (β15−66)$_2$ fragment in solution, we used size-exclusion chromatography. VLDLR(2−4)$_{HT}$, the smallest fragment with the highest affinity for (β15−66)$_2$, was selected for these experiments. When loaded separately onto a Superdex 75 column, the (β15−66)$_2$ fragment and the VLDLR(2−4)$_{HT}$ fragment were eluted at 12.1 and 12.5 mL, respectively (Figure 7). The higher mobility of (β15−66)$_2$, which has a molecular mass (10.8 kDa) lower than that of VLDLR(2−4)$_{HT}$ (14.0 kDa), was unexpected. However, it can be easily explained by the fact that (β15−66)$_2$ has unordered conformation, as was reported previously,[9] and, therefore, may have a hydrodynamic radius that is larger than that of compact VLDLR(2−4)$_{HT}$ and thus is eluted earlier. When the VLDLR(2−4)$_{HT}$ and (β15−66)$_2$ fragments were incubated together for 30 min and then loaded onto the same column, the mixture was eluted at 11.8

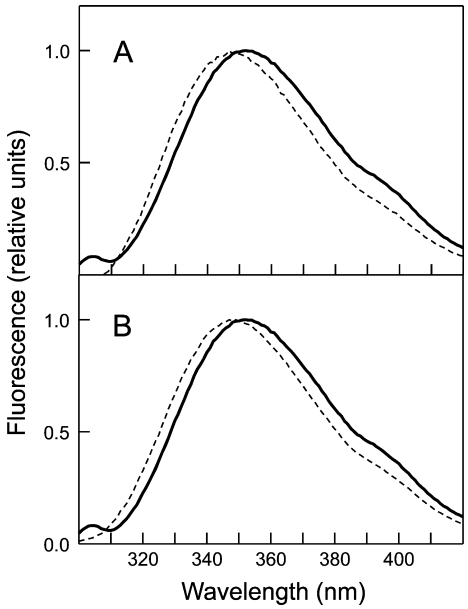

Figure 6. Fluorescence-detected interaction of the VLDLR(2−4)$_{HT}$ fragment with RAP and (β15−66)$_2$. (A) Fluorescence spectra of VLDLR(2−4)$_{HT}$ at 1 μM alone (—) or in a mixture with 1 μM RAP (---). (B) Fluorescence spectra of VLDLR(2−4)$_{HT}$ at 1 μM alone (—) or in a mixture with 10 μM (β15−66)$_2$ (---). The spectra were normalized to the intensity of VLDLR(2−4)$_{HT}$ alone taken as 1.0 in both cases. All experiments were performed at room temperature in TBS containing 1 mM $CaCl_2$.

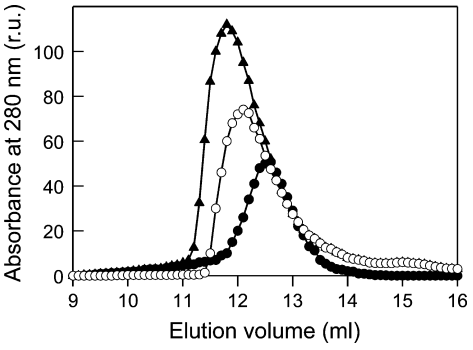

Figure 7. Size-exclusion chromatography of the VLDLR(2−4)$_{HT}$ and (β15−66)$_2$ fragments and their mixture. Elution profiles of VLDLR(2−4)$_{HT}$ loaded onto a Superdex 75 column at 2 μM, (β15−66)$_2$ loaded at 20 μM, and their mixture are shown with filled circles, empty circles, and filled triangles, respectively; the absorbance at 280 nm is presented in relative units (r.u.). The mixture containing 2 μM VLDLR(2−4)$_{HT}$ and 20 μM (β15−66)$_2$ was incubated for 30 min at 37 °C prior to being loaded onto the column. All experiments were performed at room temperature in TBS containing 1 mM Ca^{2+}.

DOI: 10.1021/acs.biochem.5b00582
Biochemistry 2015, 54, 4751−4761

mL, i.e., ahead of the individual components. These results further confirm formation of the complex between VLDLR(2−4)$_{HT}$ and (β15−66)$_2$ in solution.

Effect of the Trp^{105} to Ala Mutation on the Interaction of VLDLR(1−8)$_{HT}$ with (β15−66)$_2$. Our fluorescence studies described above, which revealed a short-wave shift of the fluorescence spectra upon formation of the complexes, suggested that Trp residues of VLDLR CR domains contribute to the interaction with the (β15−66)$_2$ fragment. To test this suggestion, we prepared a mutant of the VLDLR(1−8)$_{HT}$ fragment in which the Trp^{105} residue of its third CR domain was replaced with Ala and confirmed its proper folding by the procedures described above for other recombinant fragments. Next, we compared binding of this mutant to the (β15−66)$_2$ fragment with that of wild-type VLDLR(1−8)$_{HT}$. In ELISA experiments, when increasing concentrations of both VLDLR fragments (up to 100 nM) were added to immobilized (β15−66)$_2$, the wild-type fragment exhibited significant binding while the mutant fragment failed to bind (Figure 8). These results directly confirm the involvement of Trp residue(s) of VLDLR in the interaction with the (β15−66)$_2$ fragment.

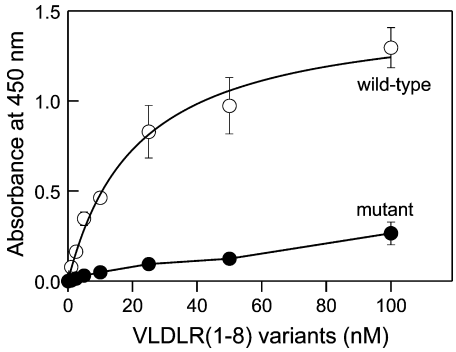

Figure 8. ELISA-detected interaction of the wild-type and mutant VLDLR(1−8)$_{HT}$ fragments with the (β15−66)$_2$ fragment. Increasing concentrations of wild-type VLDLR(1−8)$_{HT}$ (○) or VLDLR(1−8)$_{HT}$ Trp105Ala mutant (●) were incubated with microtiter wells coated with (β15−66)$_2$, and the bound fragments were detected with anti-His tag mAb, as described in Experimental Procedures. The curve for VLDLR(1−8)$_{HT}$ represents the best fit of the data to eq 1, and the determined K_d value was 21 ± 3 nM; error bars represent the standard deviation of triplicate determinations. The experiments were performed in ELISA binding buffer.

DISCUSSION

Our recent study identified VLDLR as a novel endothelial cell receptor for fibrin and revealed that interaction between fibrin and the VLDL receptor promotes leukocyte transmigration and thereby inflammation.[5] The major goals of our current studies are to establish the molecular mechanism underlying this interaction and develop its specific inhibitors that may control fibrin-dependent inflammation. We have already established that fibrin interacts with the VLDL receptor with a very high affinity and this interaction occurs exclusively through the fibrin βN domains.[5] In the study presented here, we have made the next step toward these goals by identifying domains in the VLDL receptor that are involved in the interaction with fibrin and demonstrating formation of a complex between the recombinant fragments containing fibrin-binding domains of VLDLR and VLDLR-binding domains of fibrin.

To localize the fibrin-binding site, we expressed a number of VLDLR fragments and tested their interaction with the (β15−66)$_2$ fragment mimicking a pair of the VLDLR-binding βN domains of fibrin. Because most of the fragments except sVLDLR$_{HT}$ and des(1−8)VLDLR$_{HT}$ were expressed in the bacterial expression system and each of their CR domains contains six Cys residues involved in the formation of three disulfide bonds, the major challenge was to refold these fragments and confirm that they form the proper conformation after refolding. Our attempts to test the folding status of the refolded fragments by circular dichroism (CD) were unsuccessful because their CD spectra turned out to be similar to those of unfolded proteins (results not shown). This is in agreement with the results obtained by others with CR domain-containing fragments of the LDL receptor, which were folded, but their CD spectra indicated the absence of ordered secondary structure.[31,32] Because five of eight CR domains of VLDLR contain Trp residues that may be reporters of a folded conformation, we used fluorescence spectroscopy to characterize the folding status of the expressed and refolded fragments. The results obtained by this technique clearly indicate that all VLDLR fragments prepared for this study were properly folded.

Our binding studies revealed that VLDLR(2−3)$_{HT}$ containing the second and third CR domains of VLDLR is the smallest recombinant fragment preserving high affinity for (β15−66)$_2$. This finding is not surprising because a number of previous studies revealed that at least a pair of CR domains is required for the interaction of some members of LDL receptor family with their ligands. For example, it was shown that CR domains 5 and 6 of LRP cluster II compose a minimal RAP-binding unit of this receptor and no single CR domain of this cluster shows high affinity binding for RAP.[33,34] It was also shown that three CR domains in the same cluster II of LRP, domains 5−7, constitute the complete binding site for α_2-macroglobulin.[28] The third domain of RAP also binds to a pair of CR domains of the LDL receptor, domains 3 and 4.[35] Finally, it was shown that CR domains 2 and 3 of the VLDL receptor are involved in binding with human rhinovirus type 2 (HRV2).[36,37] Thus, our data indicate that the fibrin-binding site of the VLDL receptor is formed by its second and third CR domains. In addition, the fourth CR domain of VLDLR also seems to be involved in fibrin binding because the affinity of the VLDLR(2−4)$_{HT}$ fragment for (β15−66)$_2$ was found to be approximately 2 times higher than that of VLDLR(2−3)$_{HT}$.

It should be noted that the fibrin-binding CR domains 2 and 3 of the VLDL receptor are the same domains that are involved in the interaction with HRV2. The crystal structure of a complex between this rinovirus and a fragment containing these two domains has been reported.[38] In this structure, individual CR domain 3 is bound to HRV2 through a well-defined interacting surface that includes acidic calcium-chelating residues and, in particular, an exposed Trp residue that is highly conserved in most CR domains.[38] Our fluorescence experiments (Table 2) indicate the involvement of the Trp residue of the CR domains of VLDLR in the interaction with fibrin. Such involvement was directly confirmed by mutation of the Trp residue in the third CR domain of VLDLR, which resulted in a significant loss of the affinity of VLDLR(1−8)$_{HT}$ for (β15−66)$_2$ (Figure 8). These findings suggest that interaction of fibrin with the VLDLR CR domains may occur through a mechanism similar to that reported for HRV2−VLDLR interaction.[38] They may also provide an explanation for the increased affinity of the VLDLR(2−4)$_{HT}$ fragment for

DOI: 10.1021/acs.biochem.5b00582
Biochemistry 2015, 54, 4751−4761

$(\beta 15-66)_2$ in comparison with that of VLDLR$(2-3)_{HT}$. Namely, the highly conserved Trp in the fourth CR domain of VLDLR is replaced with Phe, and this replacement may significantly decrease the affinity of this domain for fibrin. Alternatively, this replacement may eliminate fibrin binding, and the role of the fourth CR domain may be to stabilize the structure of the second and third CR domains in a conformation that is most favorable for high-affinity binding. Structural studies are required to select between these alternatives. In this respect, our demonstration of formation of a complex between free $(\beta 15-66)_2$ and VLDLR fragments in solution confirms the feasibility of studying such complexes by NMR.

In summary, the results of this study revealed that the fibrin-binding site of the VLDL receptor is formed by the structures located in its second and third CR domains and its fourth CR domain is required for the maximal affinity of this receptor for fibrin. These results provide important information for the development of specific antagonists of fibrin−VLDLR interaction that may represent novel anti-inflammatory agents for the treatment of inflammation-related cardiovascular diseases. The results also indicate the involvement of highly conserved Trp residues of VLDLR CR domains in the interaction with fibrin. The detailed molecular mechanism underlying this interaction and the exact role of the fourth CR domain in fibrin binding remain to be established.

AUTHOR INFORMATION

Corresponding Author

*University of Maryland School of Medicine, 800 W. Baltimore St., Baltimore, MD 21201. Telephone: +1 410 706 8065. Fax: +1 410 706 8121. E-mail: Lmedved@som.umaryland.edu.

Funding

This work was supported by National Institutes of Health Grant HL056051 to L.M.

Notes

The authors declare no competing financial interest.

ABBREVIATIONS

VLDLR, very low density lipoprotein (VLDL) receptor; RAP, receptor-associated protein; mAb, monoclonal antibody; CR domain, complement-type repeat domain; ELISA, enzyme-linked immunosorbent assay; SPR, surface plasmon resonance; TBS, Tris-buffered saline containing 20 mM Tris (pH 7.4) and 150 mM NaCl.

REFERENCES

(1) Languino, L. R., Plescia, J., Duperray, A., Brian, A. A., Plow, E. F., Geltosky, J. E., and Altieri, D. C. (1993) Fibrinogen mediates leukocyte adhesion to vascular endothelium through an ICAM-1-dependent pathway. *Cell 73*, 1423−1434.

(2) Altieri, D. C. (1999) Regulation of leukocyte-endothelium interaction by fibrinogen. *Thromb. Haemost. 82*, 781−786.

(3) Petzelbauer, P., Zacharowski, P. A., Miyazaki, Y., Friedl, P., Wickenhauser, G., Castellino, F. J., Gröger, M., Wolff, K., and Zacharowski, K. (2005) The fibrin-derived peptide Bβ15−42 protects the myocardium against ischemia-reperfusion injury. *Nat. Med. 11*, 298−304.

(4) Zacharowski, K., Zacharowski, P., Reingruber, S., and Petzelbauer, P. (2006) Fibrin(ogen) and its fragments in the pathophysiology and treatment of myocardial infarction. *J. Mol. Med. 84*, 469−477.

(5) Yakovlev, S., Mikhailenko, I., Cao, C., Zhang, L., Strickland, D. K., and Medved, L. (2012) Identification of VLDLR as a novel endothelial cell receptor for fibrin that modulates fibrin-dependent trans-endothelial migration of leukocytes. *Blood 119*, 637−644.

(6) Henschen, A., and McDonagh, J. (1986) Fibrinogen, fibrin and factor XIII. In *Blood Coagulation* (Zwaal, R. F. A., and Hemker, H. C., Eds.) pp 171−241, Elsevier Science Publishers, Amsterdam.

(7) Medved, L., and Weisel, J. W. (2009) on behalf of Fibrinogen and Factor XIII Subcommittee of the Scientific Standardization Committee of the International Society on Thrombosis and Haemostasis. Recommendations for nomenclature on fibrinogen and fibrin. *J. Thromb. Haemostasis 7*, 355−359.

(8) Kollman, J. M., Pandi, L., Sawaya, M. R., Riley, M., and Doolittle, R. F. (2009) Crystal structure of human fibrinogen. *Biochemistry 48*, 3877−3886.

(9) Gorlatov, S., and Medved, L. (2002) Interaction of fibrin(ogen) with the endothelial cell receptor VE-cadherin: mapping of the receptor-binding site in the NH_2-terminal portions of the fibrin β chains. *Biochemistry 41*, 4107−4116.

(10) Bach, T. L., Barsigian, C., Yaen, C. H., and Martinez, J. (1998) Endothelial cell VE-cadherin functions as a receptor for the β15−42 sequence of fibrin. *J. Biol. Chem. 273*, 30719−30728.

(11) Martinez, J., Ferber, A., Bach, T. L., and Yaen, C. H. (2001) Interaction of fibrin with VE-cadherin. *Ann. N. Y. Acad. Sci. 936*, 386−405.

(12) Yakovlev, S., Gao, Y., Cao, C., Chen, L., Strickland, D. K., Zhang, L., and Medved, L. (2011) Interaction of fibrin with VE-cadherin and anti-inflammatory effect of fibrin-derived fragments. *J. Thromb. Haemostasis 9*, 1847−1855.

(13) Wyne, K. L., Pathak, K., Seabra, M. C., and Hobbs, H. H. (1996) Expression of the VLDL receptor in endothelial cells. *Arterioscler., Thromb., Vasc. Biol. 16*, 407−415.

(14) Takahashi, S., Sakai, J., Fujino, T., Hattori, H., Zenimaru, Y., Suzuki, J., Miyamori, I., and Yamamoto, T. T. (2004) The very low-density lipoprotein (VLDL) receptor: characterization and functions as a peripheral lipoprotein receptor. *J. Atheroscler. Thromb. 11*, 200−208.

(15) Lillis, A. P., Van Duyn, L. B., Murphy-Ullrich, J. E., and Strickland, D. K. (2008) LDL receptor-related protein 1: unique tissue-specific functions revealed by selective gene knockout studies. *Physiol. Rev. 88*, 887−918.

(16) Takahashi, S., Kawarabayasi, Y., Nakai, T., Sakai, J., and Yamamoto, T. (1992) Rabbit very low density lipoprotein receptor: a low density lipoprotein receptor-like protein with distinct ligand specificity. *Proc. Natl. Acad. Sci. U. S. A. 89*, 9252−9256.

(17) Sakai, J., Hoshino, A., Takahashi, S., Miura, Y., Ishii, H., Suzuki, H., Kawarabayasi, Y., and Yamamoto, T. (1994) Structure, chromosome location, and expression of the human very low density lipoprotein receptor gene. *J. Biol. Chem. 269*, 2173−2182.

(18) Trommsdorff, M., Gotthardt, M., Hiesberger, T., Shelton, J., Stockinger, W., Nimpf, J., Hammer, R. E., Richardson, J. A., and Herz, J. (1999) Reeler/Disabled-like disruption of neuronal migration in knockout mice lacking the VLDL receptor and ApoE receptor 2. *Cell 97*, 689−701.

(19) Herz, J., and Chen, Y. (2006) Reelin, lipoprotein receptors and synaptic plasticity. *Nat. Rev. Neurosci. 7*, 850−859.

(20) Hembrough, T. A., Ruiz, J. F., Swerdlow, B. M., Swartz, G. M., Hammers, H. J., Zhang, L., Plum, S. M., Williams, M. S., Strickland, D. K., and Pribluda, V. S. (2004) Identification and characterization of a very low density lipoprotein receptor-binding peptide from tissue factor pathway inhibitor that has antitumor and antiangiogenic activity. *Blood 103*, 3374−3380.

(21) Yakovlev, S., and Medved, L. (2009) Interaction of fibrin(ogen) with the endothelial cell receptor VE-cadherin: localization of the fibrin-binding site within the third extracellular VE-cadherin domain. *Biochemistry 48*, 5171−5179.

(22) Williams, S. E., Ashcom, J. D., Argraves, W. S., and Strickland, D. K. (1992) A novel mechanism for controlling the activity of α_2-macroglobulin receptor/low density lipoprotein receptor-related protein. Multiple regulatory sites for 39-kDa receptor-associated protein. *J. Biol. Chem. 267*, 9035−9040.

DOI: 10.1021/acs.biochem.5b00582
Biochemistry 2015, 54, 4751−4761

(23) Ruiz, J., Kouiavskaia, D., Migliorini, M., Robinson, S., Saenko, E. L., Gorlatova, N., Li, D., Lawrence, D., Hyman, B. T., Weisgraber, K. H., and Strickland, D. K. (2005) The apoE isoform binding properties of the VLDL receptor reveal marked differences from LRP and the LDL receptor. *J. Lipid Res. 46*, 1721−1731.
(24) Stefansson, S., Su, E. J., Ishigami, S., Cale, J. M., Gao, Y., Gorlatova, N., and Lawrence, D. A. (2007) The contributions of integrin affinity and integrin-cytoskeletal engagement in endothelial and smooth muscle cell adhesion to vitronectin. *J. Biol. Chem. 282*, 15679−15689.
(25) Gorlatova, N., Chao, K., Pal, L. R., Araj, R. H., Galkin, A., Turko, I., Moult, J., and Herzberg, O. (2011) Protein characterization of a candidate mechanism SNP for Crohn's disease: the macrophage stimulating protein R689C substitution. *PLoS One 6*, e27269.
(26) Hembrough, T. A., Ruiz, J. F., Papathanassiu, A. E., Green, S. J., and Strickland, D. K. (2001) Tissue factor pathway inhibitor inhibits endothelial cell proliferation via association with the very low density lipoprotein receptor. *J. Biol. Chem. 276*, 12241−12248.
(27) Mikhailenko, I., Considine, W., Argraves, K. M., Loukinov, D., Hyman, B. T., and Strickland, D. K. (1999) Functional domains of the very low density lipoprotein receptor: molecular analysis of ligand binding and acid-dependent ligand dissociation mechanisms. *J. Cell Sci. 112*, 3269−3281.
(28) Dolmer, K., and Gettins, P. G. (2006) Three complement-like repeats compose the complete α_2-macroglobulin binding site in the second ligand binding cluster of the low density lipoprotein receptor-related protein. *J. Biol. Chem. 281*, 34189−34196.
(29) Battey, F. D., Gåfvels, M. E., FitzGerald, D. J., Argraves, W. S., Chappell, D. A., Strauss, J. F., 3rd, and Strickland, D. K. (1994) The 39-kDa receptor-associated protein regulates ligand binding by the very low density lipoprotein receptor. *J. Biol. Chem. 269*, 23268−23273.
(30) Jensen, J. K., Dolmer, K., Schar, C., and Gettins, P. G. (2009) Receptor-associated protein (RAP) has two high-affinity binding sites for the low-density lipoprotein receptor-related protein (LRP): consequences for the chaperone functions of RAP. *Biochem. J. 421*, 273−282.
(31) Daly, N. L., Scanlon, M. J., Djordjevic, J. T., Kroon, P. A., and Smith, R. (1995) Three-dimensional structure of a cysteine-rich repeat from the low-density lipoprotein receptor. *Proc. Natl. Acad. Sci. U. S. A. 92*, 6334−6338.
(32) Bieri, S., Atkins, A. R., Lee, H. T., Winzor, D. J., Smith, R., and Kroon, P. A. (1998) Folding, calcium binding, and structural characterization of a concatemer of the first and second ligand-binding modules of the low-density lipoprotein receptor. *Biochemistry 37*, 10994−11002.
(33) Andersen, O. M., Christensen, L. L., Christensen, P. A., Sorensen, E. S., Jacobsen, C., Moestrup, S. K., Etzerodt, M., and Thogersen, H. S. (2000) Identification of the minimal functional unit in the low density lipoprotein receptor-related protein for binding the receptor-associated protein (RAP). A conserved acidic residue in the complement-type repeats is important for recognition of RAP. *J. Biol. Chem. 275*, 21017−21024.
(34) Andersen, O. M., Schwarz, F. P., Eisenstein, E., Jacobsen, C., Moestrup, S. K., Etzerodt, M., and Thogersen, H. C. (2001) Dominant thermodynamic role of the third independent receptor binding site in the receptor-associated protein RAP. *Biochemistry 40*, 15408−15417.
(35) Fisher, C., Beglova, N., and Blacklow, S. C. (2006) Structure of an LDLR-RAP complex reveals a general mode for ligand recognition by lipoprotein receptors. *Mol. Cell 22*, 277−283.
(36) Hewat, E. A., Neumann, E., Conway, J. F., Moser, R., Ronacher, B., Marlovits, T. C., and Blaas, D. (2000) The cellular receptor to human rhinovirus 2 binds around the 5-fold axis and not in the canyon: a structural view. *EMBO J. 19*, 6317−6325.
(37) Neumann, E., Moser, R., Snyers, L., Blaas, D., and Hewat, E. A. (2003) A cellular receptor of human rhinovirus type 2, the very-low-density lipoprotein receptor, binds to two neighboring proteins of the viral capsid. *J. Virol. 77*, 8504−8511.
(38) Verdaguer, N., Fita, I., Reithmayer, M., Moser, R., and Blaas, D. (2004) X-ray structure of a minor group human rhinovirus bound to a fragment of its cellular receptor protein. *Nat. Struct. Mol. Biol. 11*, 429−434.

DOI: 10.1021/acs.biochem.5b00582
Biochemistry 2015, 54, 4751−4761